

We are IntechOpen, the world's leading publisher of Open Access books Built by scientists, for scientists

6,900

Open access books available

186,000

International authors and editors

200M

Downloads

Our authors are among the

154

Countries delivered to

TOP 1%

most cited scientists

12.2%

Contributors from top 500 universities



WEB OF SCIENCE™

Selection of our books indexed in the Book Citation Index
in Web of Science™ Core Collection (BKCI)

Interested in publishing with us?
Contact book.department@intechopen.com

Numbers displayed above are based on latest data collected.
For more information visit www.intechopen.com



Broadband Slotted Waveguide Array Antenna

Yogesh Tyagi and Pratik Mevada

Additional information is available at the end of the chapter

<http://dx.doi.org/10.5772/intechopen.78308>

Abstract

This chapter describes the design and development of broadband slotted waveguide array (SWA) antenna. Conventional SWA antenna offers a few percentages of bandwidth, which can be enhanced using proposed novel differential feeding technique which electrically divides large resonating SWA into wideband subarrays by creating virtual shorts. This chapter discusses concepts to achieve broadband nature of SWA antennas, design, development, and characterization of edge fed slotted waveguide array antenna, coupling slot fed SWA antenna, and high efficiency broadband slotted waveguide array. The developed SWA antennas are characterized and their measured results are presented. The developed prototype of proposed SWA antenna demonstrates measured return loss better than -17 dB over 7.6% bandwidth and achieves 90.2% antenna efficiency. This chapter also briefs about planar broadband SWA antenna and its prototype development and characterization.

Keywords: slotted waveguide array, broadband antenna, array antenna, high efficiency antenna, virtual short, coupling slot

1. Introduction

Slotted waveguide array (SWA) antenna technology has been utilized by many spaceborne missions such as Radarsat-1, SIR-X, ERS-1/2, and Sentinel-1, because SWA technology has several advantages like high efficiency, good mechanical strength, high power handling capacity, and manufacturing ease. However, the main drawback of this technology is narrow impedance bandwidth, which limits its applications to support high resolution SAR systems for civil and military applications. Moreover, the traveling wave type SWA provides wide bandwidth, but its efficiency is very low.

Various bandwidth improvement techniques have been explored and reported in the literature, which includes reducing waveguide wall thickness, reducing waveguide cross section, widening slot width, and modifying slot shapes, e.g., dumbbell shape and elliptical shape [1–4]. When SWA is targeted for space applications, the reduction in wall thickness may not be suitable as it has to survive severe vibration and thermal loads. When SWA is targeted for high power and low attenuation systems, the reduction in waveguide cross section shows inferior performance. Moreover, slot widening and slot shaping affect the cross-polarization performance. SWA with modified slot shapes also needs high manufacturing accuracy. Although these techniques provide bandwidth improvement, other antenna parameters are compromised due to the constraints of respective techniques.

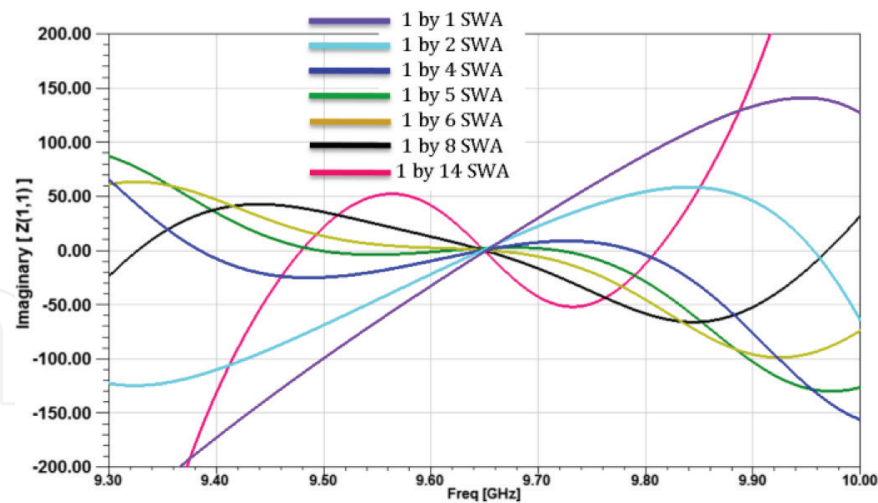
Sub-arraying technique is widely used and considered as most effective to broaden the bandwidth of conventional SWA. In this technique, SWA is divided into subarrays [3], so that better control over variation of normalized impedance (z) or admittance (y) with frequency is achieved. Generally, coupling slots are used to feed these subarrays. Being the resonating structure, coupling slot restricts the bandwidth performance. Therefore, a novel differential feeding technique has been presented to remove the constraints introduced by coupling slots. WR-90 (22.86 mm \times 10.16 mm in cross section) waveguide has been selected and the design of broadband SWA has been carried out at 9.65 GHz center frequency. Design and demonstration of SWA with conventional feeding techniques, i.e., edge feeding and coupling slot feeding have also been discussed and compared with proposed broadband SWA design.

In this chapter, Section 2 discusses the conventional bandwidth enhancement approach and various feeding mechanisms of subarrays are followed in Section 3. Mathematical proof of the presence of virtual short created due to the proposed differential feeding technique has been discussed in Section 4. Design and simulation of 10 elements linear SWAs is outlined in Section 5. Design of linear array is extended to planar array and it is presented in Section 6. The measured results of developed prototypes are provided in Section 7 with brief discussion.

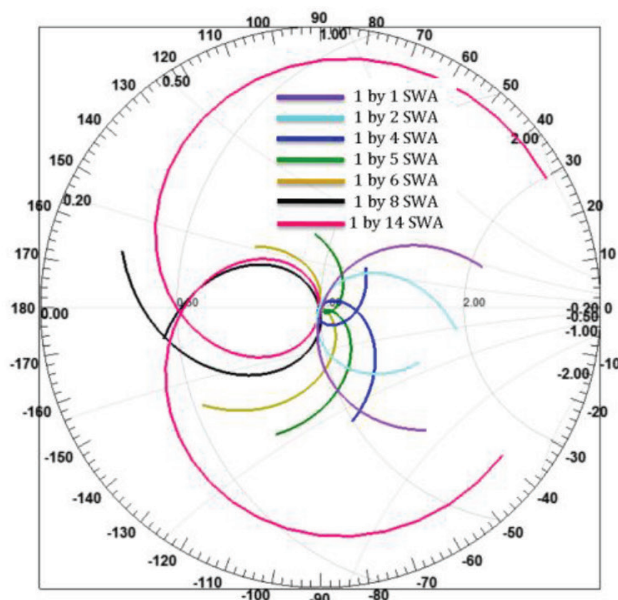
2. Subarray: conventional technique for bandwidth enhancement

Many techniques have been discussed in the literature to enhance the bandwidth of traditional slotted waveguide array antenna. As it has been discussed in the previous section, the use of thin wall waveguides, reduced cross sectional waveguide, wide slots, and modified slot shapes are the reported techniques to improve the bandwidth. However, these techniques are capable to improve few percent of bandwidth. Hence, they are not suitable to achieve expected wideband performance.

Fundamentally, the bandwidth enhancement can be achieved by reducing the reactive effects of the input admittance over the frequency band of interest. By proper selection of number of slot elements in the edge fed linear SWA antenna for the required bandwidth, nearly zero reactive part of input admittance can be obtained for the desired frequency band, which subsequently results in wide bandwidth performance. **Figure 1(a)** shows the case study of variation of reactive part of input admittance with frequency for different number of slots in a single



(a)



(b)

Figure 1. (a) Variation of reactive component of input admittance for different number of longitudinal slots and (b) variations of different number of longitudinal slots using smith chart.

branch of WR-90 waveguide. From **Figure 1(a)**, it can be observed that reactive part is very high and crosses zero at 9.65 GHz. The frequency at which zero crossing occurs is the resonance frequency of slot. When the number of slots reaches up to 6, the variation of reactive part of input admittance tends to zero over the frequency band of interest, which confirms the realizability of wideband SWA. When the number of slots is further increased, the reactive part of admittance starts to destabilize near zero and eventually provides strong resonant behavior. This phenomenon is also validated by plotting the impedance variation for different number of slots on smith chart, as shown in **Figure 1(b)**. It can be observed that varying the number of slots results in variation in impedance loop. By adjusting this impedance loop near normalized impedance of 1 by proper selection of number of slots, the antenna bandwidth can be improved.

The optimum number of radiating slots is selected by properly adjusting the size of impedance loop in smith chart. However, the bandwidth enhancement is not achieved by only size adjustment. Once the size of the impedance loop is adjusted which indicates the optimum number of radiating slots are selected, the impedance loop is moved to normalized impedance of 1 by using the impedance matching section. The impedance matching section maintains the variation of reflection coefficient below desired value, resulting in wide bandwidth performance. The discussed concept has been verified using circuit simulation in Advanced Design Studio (ADS). In this simulation, slotted waveguide array antenna having three longitudinal slots has been modeled using three parallel RLC network and inbuilt waveguide transmission line component. The circuit equivalent of three elements resonant SWAs is shown in **Figure 2(a)**. Here, slots are modeled as parallel R , L and C and they are connected by transmission line section having Z_0 and β equivalent to WR-90 waveguide at 9.6 GHz. The values of L and C have been selected such that LC network resonates at center frequency of 9.6 GHz. The value of R has been selected to provide normalized admittance of 1 at the input of the array. The circuit schematic in ADS is shown in **Figure 2(c)**. Here, separate extra impedance matching section has been added to adjust the location of impedance loop in smith chart. The return loss plot and impedance on smith chart with/without impedance matching section are presented in **Figure 3**. It can be observed that, without matching section at the input, the circuit shows highly resonating behavior. After adding matching section, the impedance loop has been shifted around the normalized impedance of 1, which results in wider impedance bandwidth.

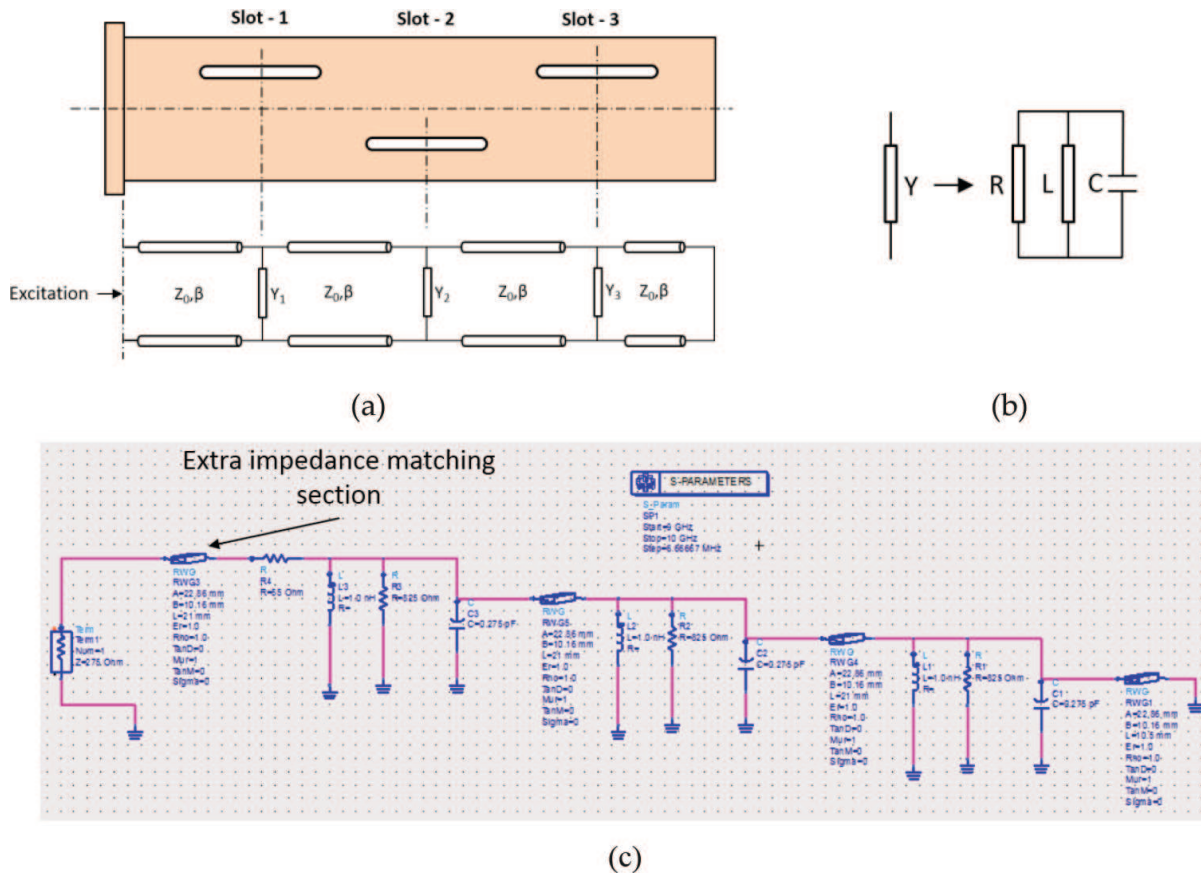


Figure 2. (a) Equivalent circuit representation of three elements resonant SWAs, (b) admittance modeling as parallel RLC, and (c) circuit layout of SWA in ADS.

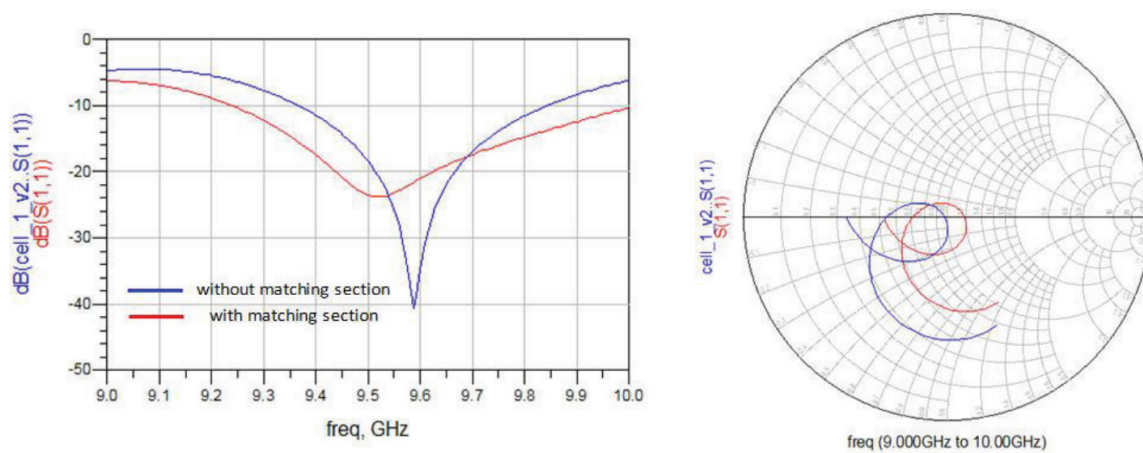


Figure 3. Simulation results of circuit layout.

In the case of slotted waveguide array antenna, the concept of impedance overloading of slots can be used as impedance matching technique to shift the impedance loop in smith chart, in place of adding extra impedance matching section. To validate the concept, five elements linear slotted waveguide array antenna has been designed as shown in **Figure 4(a)**. From **Figure 4(b)**, it can be observed that the selection of five radiating slots for the array provides optimum bandwidth.

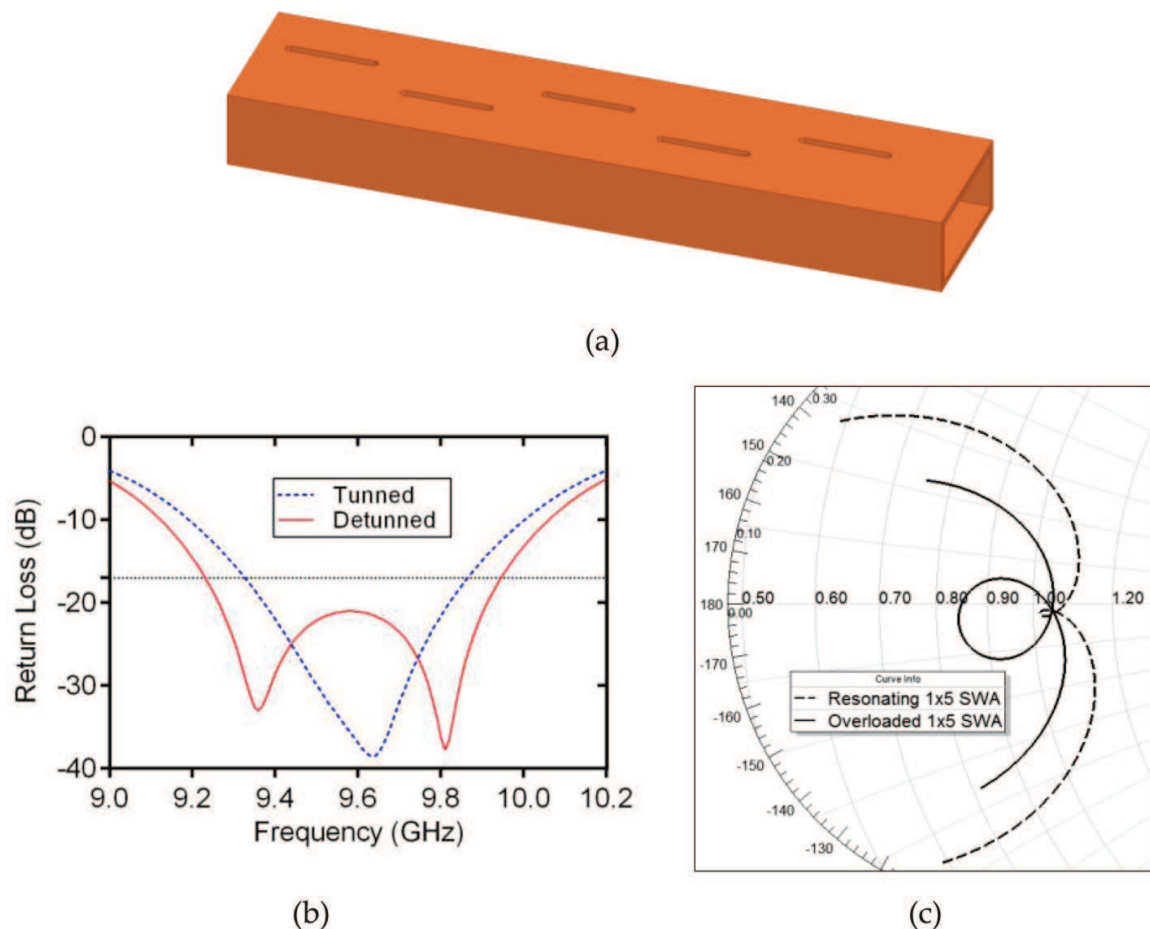


Figure 4. (a) Five elements linear slotted waveguide array antenna, (b) return loss performance, and (c) smith chart.

	Without admittance overloading	With admittance overloading
Slot admittance	$0.1945 - j*0.016$	$0.2291 - j*0.016$
Slot length	15.37	15.40
Slot offset	3.28	3.60

Table 1. Slot parameters.

Mutual coupling between the elements may be neglected due to considerably small array size. Therefore, Stevenson's formula can be used to compute slot lengths and offsets. Stevenson's formula provides the slot parameters for designed frequency only. Hence, the design of SWA with the computed slot parameters shows highly resonating nature, as shown in **Figure 4(b)**. It can be observed that the achieved return loss bandwidth is 2%. As it has been discussed earlier, the bandwidth of slotted waveguide array antenna can be improved using impedance overloading. To implement impedance over loading, slot length and offsets are tuned so that resultant admittance value slightly deviates from normalized value 1. For small SWA, this process can be carried out manually. **Table 1** lists slot admittance and their physical parameters for impedance overloading and non-overloading cases. **Figure 4(b)** shows the return loss performance of slotted waveguide array antenna incorporated with impedance overloading concept. It can be observed that the achieved return loss bandwidth is 15%, which is noteworthy improvement. Moreover, more detail about impedance overloading is explained in [4].

Furthermore, the linear array of five slots does not provide required gain, beamwidth, and desired gain ripples, if the pattern is shaped. Therefore, most effective approach to achieve overall performance of slotted waveguide array antenna is subarray approach. This technique exploits the advantages provided by dividing the large narrowband array into small wide-band array ("Subarray"). The concept of subarray and its related theoretical studies have been published in the literature. But, the physical process of bandwidth broadening using subarray is not explained in detail.

3. Feeding mechanisms for subarray

The feeding mechanism of subarrays of the slotted waveguide array antenna plays a crucial role in limiting its bandwidth performance. Conventionally, the power to each subarray branch is delivered using feeding waveguide connected with subarrays by means of coupling slots. **Figure 5** shows the geometry of the 10-element slotted waveguide array antenna excited using coupling slots. Being the resonating element, coupling slots have their own resonant behavior and hence, the variation of reactive part of input admittance with frequency. Overall antenna resulting input admittance behavior is governed by the combined effect of radiating slots and coupling slots. Therefore, inherent wide bandwidth behavior of radiation slots, achieved using sub-array technique is degraded. Furthermore, coupling slots are used in feeding section of SWA which has to handle larger power than radiation branch of waveguide. Multipaction margin is also affected as narrow gap structures (i.e., coupling

slots) which are added in the path of high power signal. These factors are the major causes to limit the use of coupling slot feeding technique for large wideband SWAs. The design and simulation of 10 elements linear SWAs excited with coupling slot has been carried out and discussed in subsequent sections.

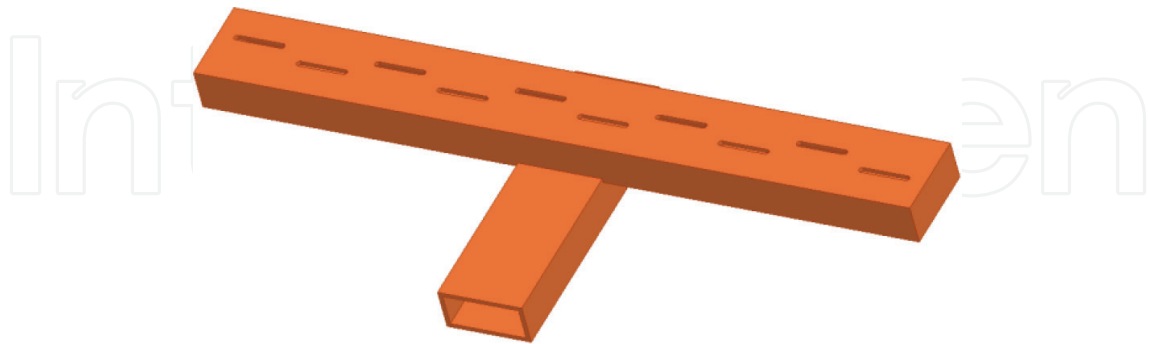


Figure 5. Geometry of 10 elements slotted waveguide array antenna fed coupling slots.

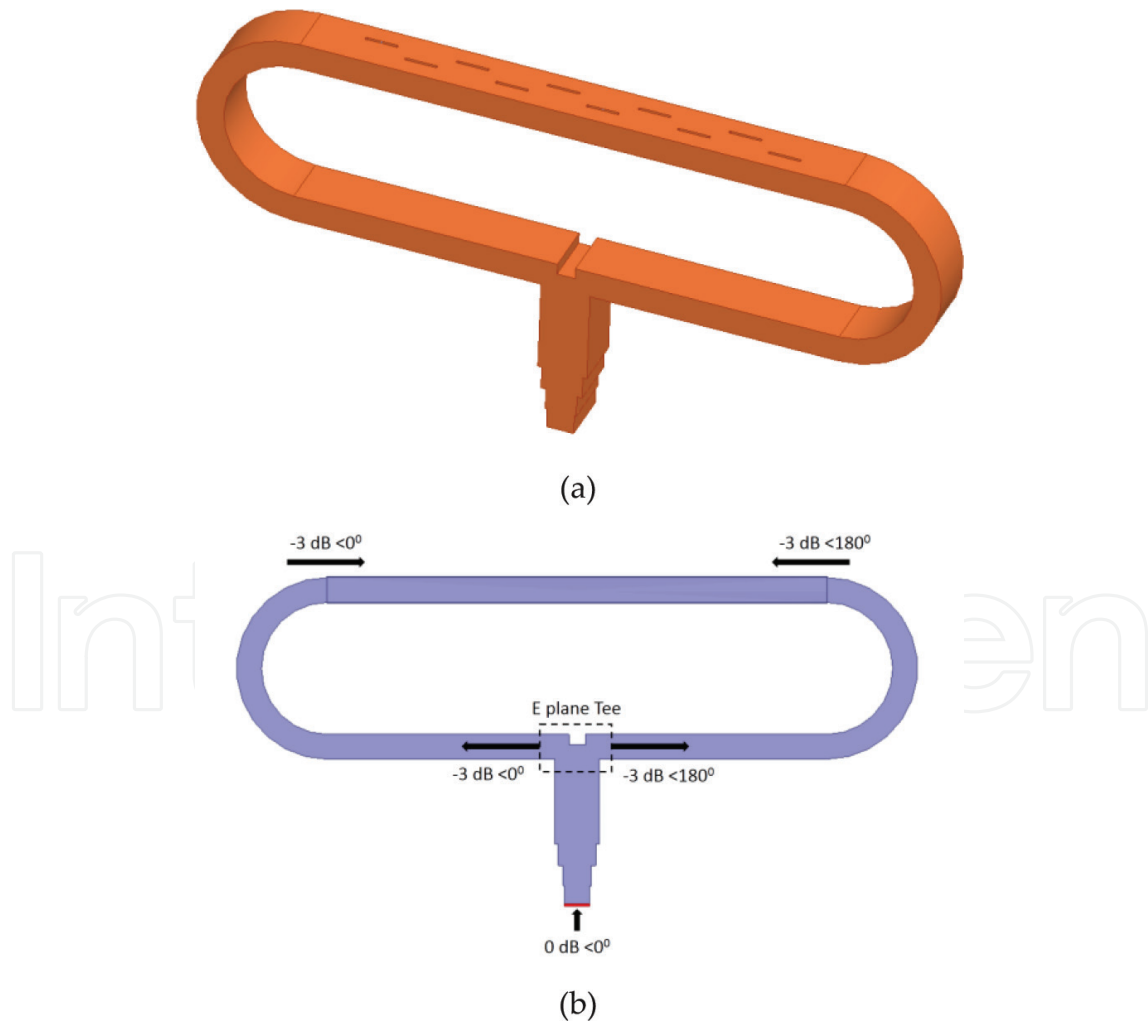


Figure 6. (a) Geometry of 10 elements slotted waveguide array antenna excited using differential feeding technique and (b) presence of virtual short.

Bandwidth and power handling performance of SWA can be preserved by eliminating resonating components from waveguide feed network design. This chapter describes the differential feeding technique which does not add any resonating structure in waveguide feeder network and maintains the effective bandwidth of subarray. **Figure 6(a)** shows the geometry of the proposed technique. Here, the edges of SWA are fed with 180° out of phase signal, which creates virtual short in the center of SWA. Presence of virtual short bifurcates the linear array and hence, effectively preserves the bandwidth achieved by subarraying. The presence of virtual short can be substantiated by observing current distribution on differentially excited waveguide, as shown in **Figure 6(b)**. The mathematical proof to validate the theory of virtual short is also detailed in Section 4. Moreover, two edges can be fed using E-plane T-junction which has inherent characteristics to provide 180° out of phase signals, irrespective of frequency of operation [5]. Therefore, the compensation of 180° phase over broadband of frequency can be achieved. Furthermore, the feeding network does not contain any resonating structures like coupling slots, to limit power handling capacity. The design and simulation results of 10 elements linear slotted waveguide array antenna incorporating the differential feeding technique is discussed in Section 5.

4. Theory of virtual short

Circuit theory has been applied to establish the virtual short theory in SWA. A branch in a circuit can be considered as short when the potential difference between two nodes of a branch is zero and the current flow is high in that branch. The presence of virtual short can be proved using similar concept in waveguide. In waveguide, E -field and H -field are used to derive the short circuit condition. The cross section of waveguide along length direction is shown in **Figure 7**. Here, operating frequency of 9.65 GHz has been selected. As WR-90 waveguide having cross sectional dimension of $(W_a = 22.86 \text{ mm}) \times (W_b = 10.16 \text{ mm})$ is used, only TE_{10} mode is supported at these frequency. As it can be seen in **Figure 7**, $Z = 0$ end is excited with $1 < 0^\circ$ and $Z = Z_l$ is excited with $1 < 180^\circ$. Therefore, E_y component of the signals is canceled and H_x components of it are added at the center of waveguide, which satisfy the short circuit condition. Here, there is no conductor at the center of waveguide. However, the short circuit condition is fulfilled, which substantiate the presence of virtual short at the center of waveguide.

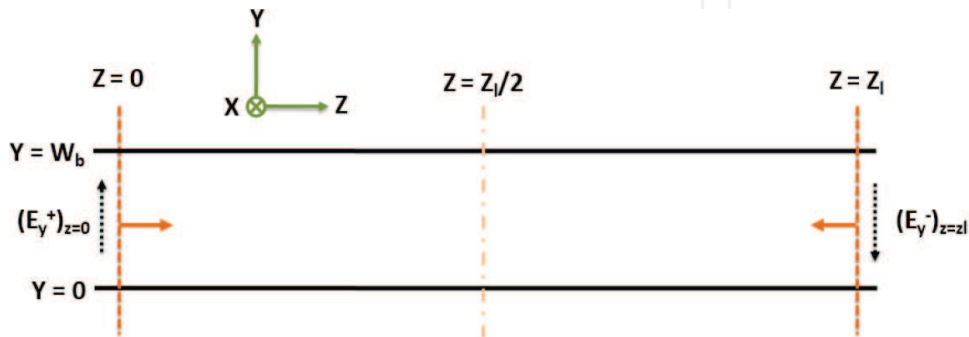


Figure 7. Cross section of WR-90 waveguide along length direction.

For TE₁₀ mode,

$$E_x^+ = 0$$

$$E_y^+ = -\frac{A_{10}}{\epsilon} \frac{\pi}{a} \sin\left(\frac{\pi x}{a}\right) e^{-j\beta_z z}$$

$$E_z^+ = 0$$

$$H_x^+ = A_{10} \frac{\beta_z}{\omega \mu \epsilon} \frac{\pi}{a} \sin\left(\frac{\pi x}{a}\right) e^{-j\beta_z z}$$

$$H_y^+ = 0$$

$$H_z^+ = -j \frac{A_{10}}{\omega \mu \epsilon} \left(\frac{\pi}{a}\right)^2 \cos\left(\frac{\pi x}{a}\right) e^{-j\beta_z z}$$

Here, excitation coefficient A_{10} for both inputs are $(A_{10})_z = 0 = 1$ and $(A_{10})_z = z_l = -1$ (180° out of phase). For E_y field component, at $z = 0$ (+ve z directed wave)

$$(E_y^+)_{z=0} = -\frac{\pi}{\epsilon a} \sin\left(\frac{\pi x}{a}\right) e^{-j\beta_z z}$$

at $z = z_l$ (-ve z directed wave)

$$(E_y^+)_{z=z_l} = \frac{\pi}{\epsilon a} \sin\left(\frac{\pi x}{a}\right) e^{-j\beta_z(z_l-z)}$$

Hence,

$$(E_{ytotal})_{z=\frac{z_l}{2}} = (E_y^+)_{z=0} + (E_y^+)_{z=z_l}$$

$$(E_{ytotal})_{z=\frac{z_l}{2}} = 0$$

Now, for H_x field component,

$$(A_{10})_z = 0 = (A_{10})_z = z_l = 1$$

$$(H_x^+)_{z=0}, (H_x^+)_{z=z_l} = \frac{\beta_z \pi}{\omega \mu \epsilon a} \sin\left(\frac{\pi x}{a}\right) e^{-j\beta_z(\frac{z_l}{2})}$$

at $z = z_l/2$.

Hence,

$$(H_{xtotal})_{z=\frac{z_l}{2}} = 2(H_x^+)_{z=0}$$

Now, for H_z field component,

$$(A_{10})_z = 0 = 1 \text{ and } (A_{10})_z = z_l = -1$$

Hence,

$$(H_{ztotal})_{z=\frac{z_l}{2}} = 0$$

Therefore,

$$(E_{ytotal})_{z=\frac{z_l}{2}} = 0$$

$$(H_{xtotal})_{z=\frac{z_l}{2}} = 2(H_x^+)_{z=0}$$

$$(H_{ztotal})_{z=\frac{z_l}{2}} = 0$$

This fulfills the condition of short circuit node.

5. Design and simulation of linear slotted waveguide array antenna

Elliot's design technique has been applied to design SWA [6–8]. Elliot's design technique synthesizes slot lengths and offsets and incorporate mutual coupling between slots. This technique uses admittance variation of isolated shunt slot as a function of slot lengths and resonant length and the offset from center. Ansys HFSS 2014 has been used to compute the admittance variation and the real and imaginary part of admittance is plotted in **Figure 8(b)** and **(c)**. These plots are fed as input to Elliot's design technique and slot lengths and offsets are synthesized such that normalized input admittance (y) obtains value '1' at center frequency 9.65 GHz. Ten-element conventional edge fed SWA using synthesized slot lengths and offsets has been designed and shown in **Figure 9**.

3D simulation of conventional edge fed SWA has been carried out and the results are presented in Section 7. Simulation shows 2.8% 17-dB impedance bandwidth which does not cater to current need of bandwidth for communication and remote sensing applications. As it has been discussed in previous sections, 10 elements array can be split into two five element arrays, which will considerably increase the return loss bandwidth. Here, five element arrays

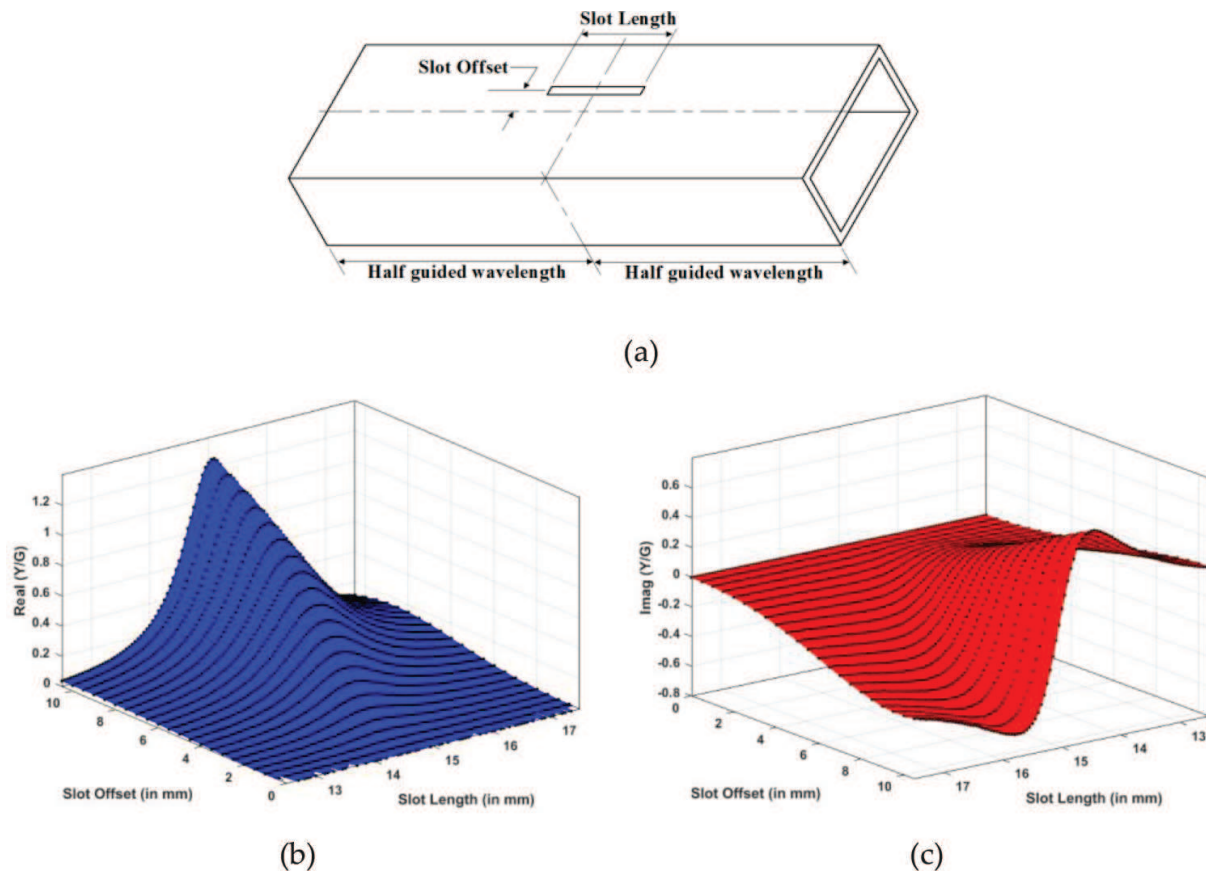


Figure 8. (a) Dimensional details of isolated shunt slot, variations of (b) real part of slot admittance, and (c) imaginary part of slot admittance functions of slot length and slot offset.

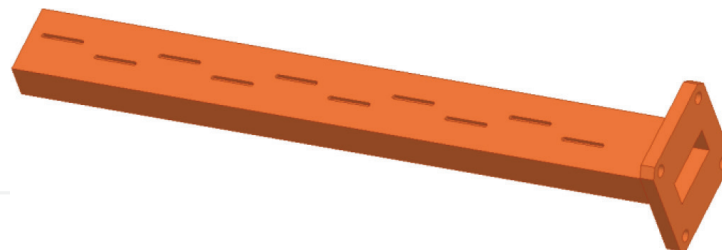


Figure 9. Geometry of conventional SWA with 15 mm slot length and 3.5 mm slot offset.

are combined in parallel. Therefore, slot lengths and offsets are to be adjusted so that normalized input impedance of each subarray becomes value '2'. Consequently, parallel combination of five element array results normalized admittance of 1 at input.

Subarrays can be excited by proper waveguide plumbing incorporated with coupling slots and waveguide tees. Such feeding network effectively governs the impedance bandwidth of SWA. In Section 3, the conventional coupling slot-based excitation technique and proposed differential feeding technique have been broadly detailed. To compare these techniques, 10-elements linear SWAs have been designed and optimized to achieve maximum bandwidth

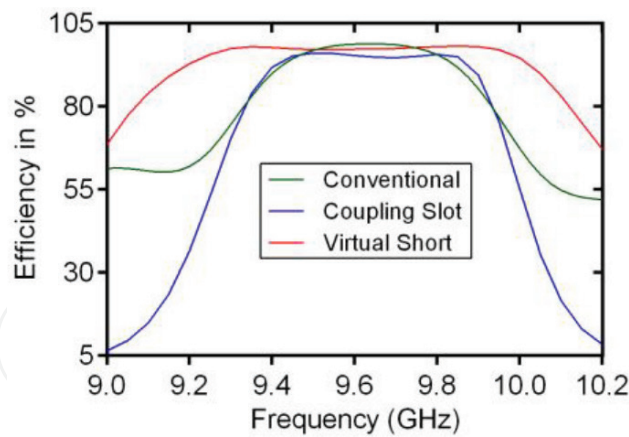


Figure 10. Comparison of total antenna efficiency between edge fed, coupling slot fed, and differential fed SWA.

for both type of feeding techniques. The simulated and their measured performances are compared and discussed in Section 7. When SWA is excited with coupling slots, 4.6% 17-dB RL bandwidth has been achieved, which is considerably less as compared to the expected bandwidth from subarray technique. The reduction in bandwidth can be ascribed to the addition of admittance variation of resonating coupling slots to the admittance variation of subarrays.

The chapter discusses the differential feeding technique which does not require resonating elements and hence, maintains the impedance bandwidth of subarray. After proper design and optimization of 10-elements linear SWAs with proposed feeding technique, 7.5% 17-dB RL bandwidth has been achieved, which is significantly large as compared to the RL bandwidth achieved when subarrays are fed using coupling slots. However, the achieved return loss bandwidth is not same as the RL bandwidth provided by a single subarray because of frequency sensitive nature of waveguide bends and E plane T junction.

Antenna efficiency is one of the important factors and it is the function of the reflection coefficient while considering other parameters constant. Therefore, if the variation of reflection coefficient with frequency is maintained below certain desired level (here, it is -17 dB), the antenna efficiency remains the same over the band of interest. Total antenna efficiency variation

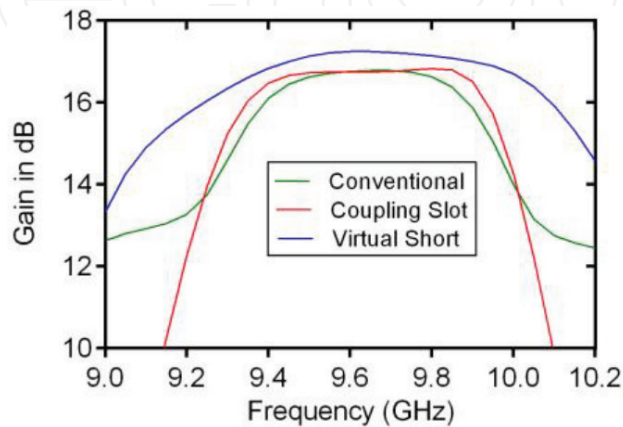


Figure 11. Comparison of realized antenna gain between edge fed, coupling slot fed, and differential fed SWA.

with frequency for various designed SWAs is shown in **Figure 10**. As it can be observed from **Figure 10**, ~90% efficiency is achieved over the band of interest for the proposed broadband SWA. Furthermore, SWA fed using coupling slots shows lowest efficiency, which can be attributed to high insertion loss added by coupling slots. **Figure 11** shows the plot of variation of realized gain with frequency for the presented SWAs. As it can be observed, the behaviors of realized gain and antenna efficiency with frequency are same. Moreover, gain flatness of proposer SWA has significant improvement as compared to conventional edge fed SWA and coupling slot fed SWA.

6. Design and simulation of planar slotted waveguide array antenna

In SWA, resonant slots are cut on the broadwall of the waveguide. Therefore, when any radiating structure working on the same band of interest is placed near these resonant slots, strong coupling between the resonant slots on waveguide and radiating structure occurs and reduces the impedance bandwidth of the SWA. This effect has been examined for the proposed broadband SWA by designing 2×10 planar broadband SWA using proposed differential feeding technique. **Figure 12** shows the design model of planar SWA. Here, two linear broadband SWAs are placed in proximity and combined using 1:2 waveguide feeder network employed with E- and H-plane tees. As it has been discussed, coupling between two linear SWAs should degrade the impedance bandwidth of planar SWA. However, proper optimization of feeder network can cancel the coupled energy, subsequently preserving the bandwidth of planar broadband SWA. About 7.8% 17-dB return loss bandwidth has been achieved in simulation. Section 7 shows the plots of simulated RL and far field patterns.

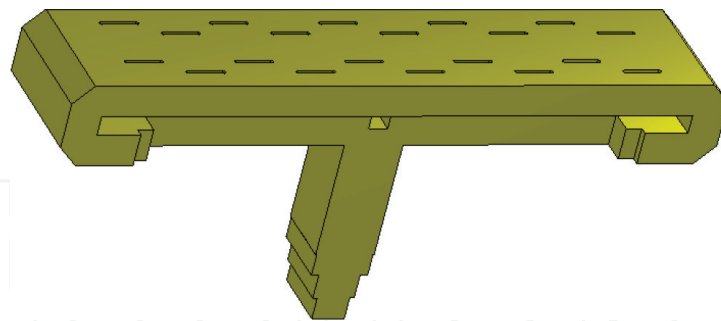


Figure 12. Geometry of 2×10 planar broadband SWA antenna with differential feeding mechanism.

7. Prototype fabrication and measurement

The presented antenna designs are fabricated and characterized for experimental validation of proposed technique. The realized prototypes of conventional SWA, SWA excited with coupling slots, and SWA with differential feeding technique are shown in **Figure 13**. Agilent E8363B microwave network analyzer with SOLT WR-09 calibration kit has been used to measure the return loss performance of these prototypes. **Figure 14** shows the comparison

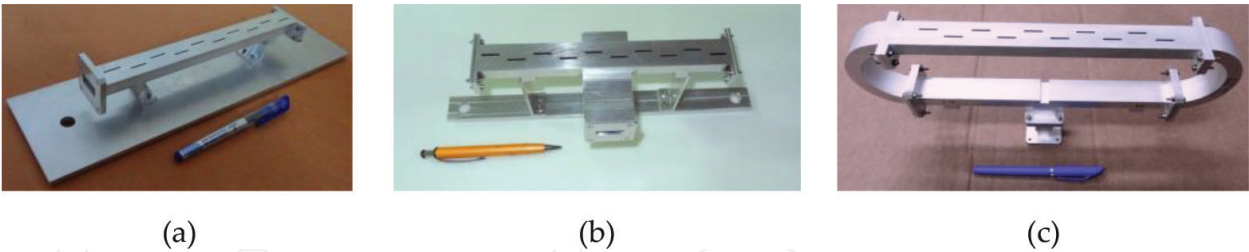


Figure 13. Fabricated structures (a) conventional slotted waveguide array, (b) slotted waveguide array antenna using coupling slots, and (c) SWA using differential feeding mechanism.

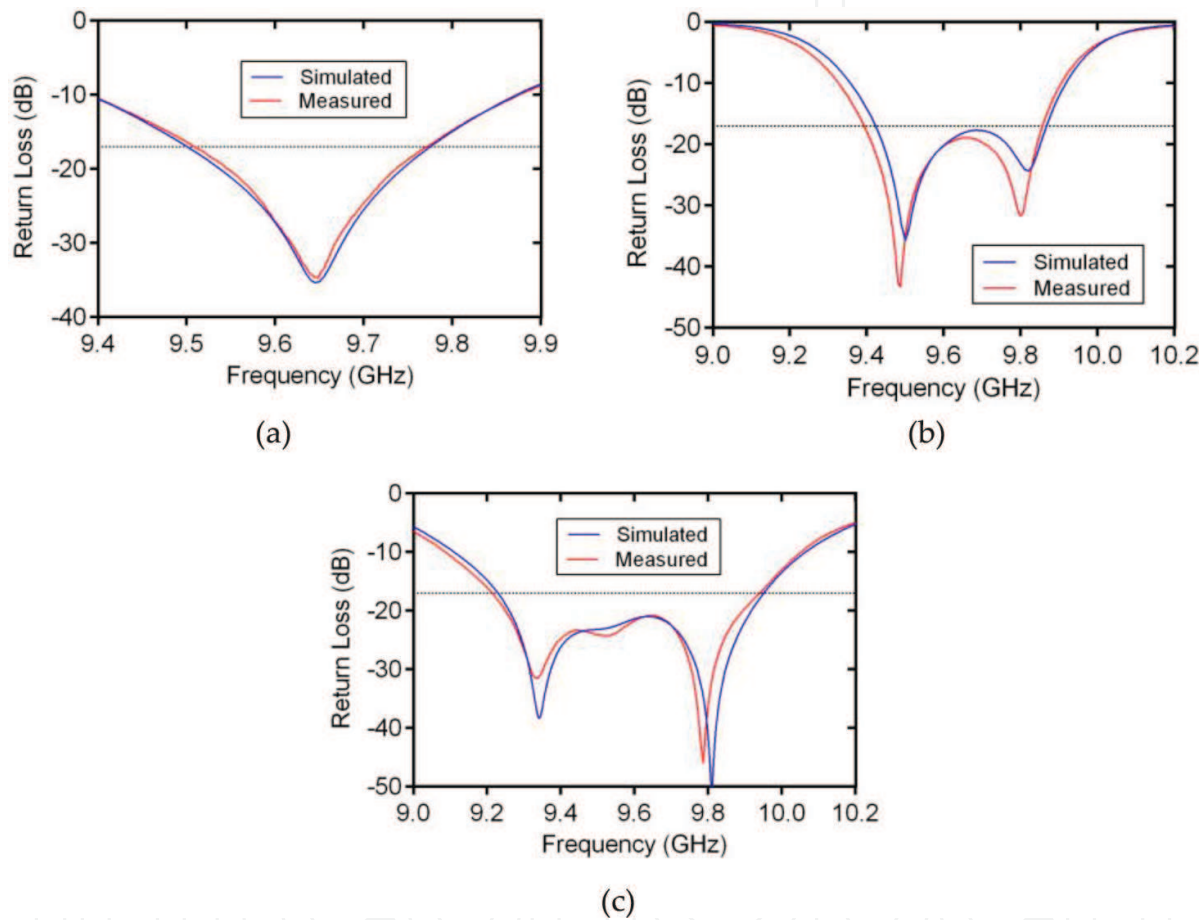


Figure 14. Simulated and measured return loss performance of (a) conventional slotted waveguide array, (b) slotted waveguide array antenna using coupling slots, and (c) SWA using differential feeding mechanism.

between measured and simulated return loss performance and **Table 3** lists the simulated and measured percentage bandwidth of each prototype. From **Figure 14**, it can be said that the simulated and measured results are in close agreement. Moreover, **Table 2** also compares the size of the fabricated SWA structure. The fabricated structures include the baseplates and interface plates which are not actual part of the antenna. They are connected with structure to perform S-parameter and far field characterization.

To validate the theory of virtual short in SWA, analysis has been carried out by placing physical short in the location of virtual short and its return loss performance is shown in **Figure 15**. No deviation from return loss performance of SWA with virtual short can be observed.

	Length (mm)	Height (mm)	Width (mm)
Conventional slotted waveguide array	36	14	50
Slotted waveguide array antenna using coupling slots	36	14	9.5
SWA using differential feeding mechanism	35	17	50

Table 2. Dimensions of fabricated SWA structures.

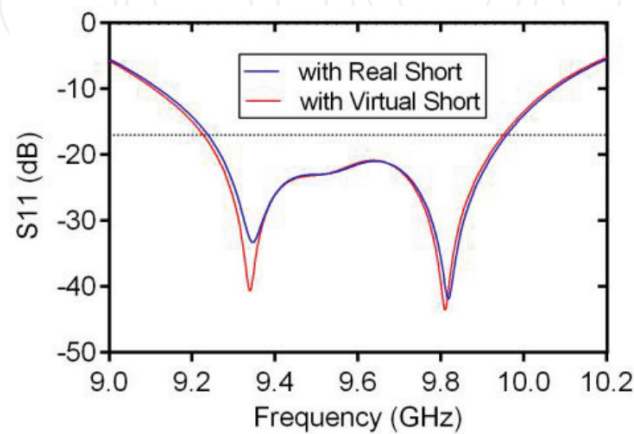


Figure 15. Simulated return loss performance of SWA with physical short and virtual short.

The radiation pattern and gain measurement of each fabricated prototype has also been carried out at in-house anechoic chamber. **Figure 16** shows proposed SWA antenna mounted on device under test (DUT) unit at anechoic chamber for far field measurement. Measured radiation patterns at 9.65 GHz for each prototype are shown in **Figure 17**. To obtain the gain of the array under test, the received power level difference between array under test and a standard gain horn has been measured and the results are presented in **Table 3** with their simulated performance. Good correlation between simulated and measurement of far-field parameters is obtained. Moreover, **Figure 18** shows the variation of measured gain with frequency of

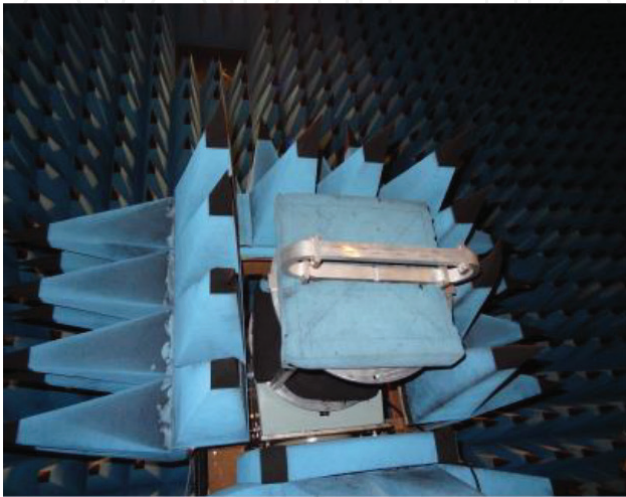


Figure 16. SWA using differential feeding mechanism mounted on DUT of anechoic chamber.

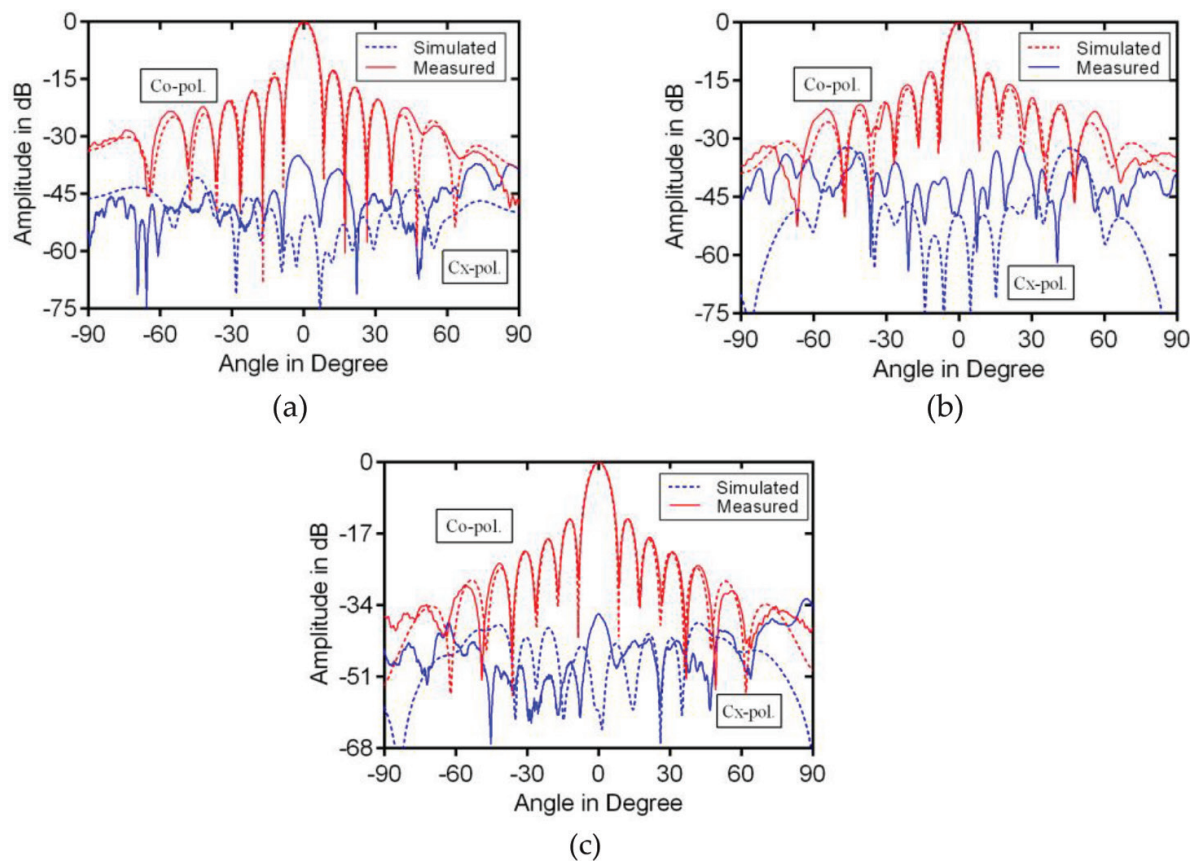


Figure 17. Simulated and measured radiation pattern of (a) conventional slotted waveguide array, (b) slotted waveguide array antenna using coupling slots, and (c) SWA using differential feeding mechanism.

9.65 GHz	Simulated BW (%)	Measured BW (%)	Simulated gain (dB)	Measured gain (dB)
Edge fed SWA	2.8	2.7	16.60	16.35
SWA fed by coupling slot	4.6	4.8	16.61	16.21
SWA fed by differential feeding mechanism	7.5	7.6	16.62	16.32

Table 3. Measured bandwidth.

SWA with differential feeding mechanism. 0.88 dB gain variation over 800 MHz frequency range has been achieved.

Moreover, another most important mechanical aspects are antenna mass and its fabrication. Although the proposed SWA has high mass as compared to conventional SWAs, it can be reduced by the optimization of waveguide feeder network while incorporating mass as important factor in cost function and by using CFR- (Carbon Fiber Reinforced Plastic) based waveguides. In addition, the proposed SWA is complex to fabricate as compared to conventional SWAs. But, the recent evolution in mechanical fabrication processes has expanded the scope of fabricating complex waveguide structure within desired mass.

A prototype of 2×10 planar SWA antenna has also been realized and characterized to verify the simulation data. The developed prototype model is shown in **Figure 19** and its measured RL performance and far field pattern with their simulation data is plotted in **Figures 20** and **21**.

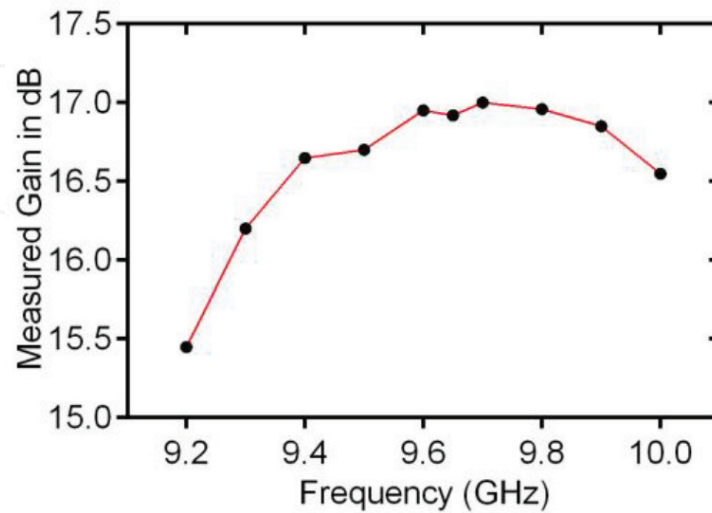


Figure 18. Variation of measured gain with frequency for SWA with differential feeding mechanism.



Figure 19. Fabricated structures of 2×10 planar SWA using differential feeding mechanism.

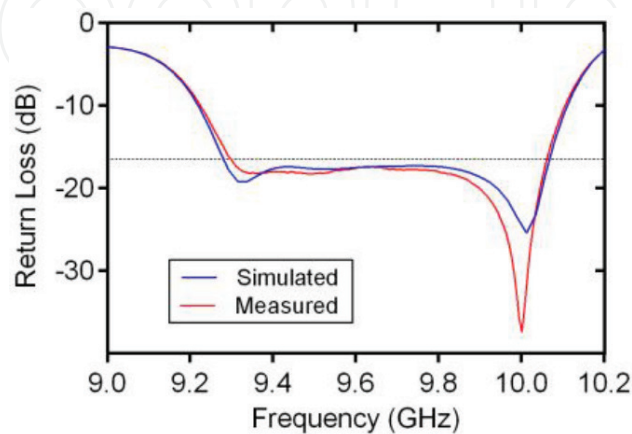


Figure 20. Simulated and measured return loss performance of 2×10 planar SWA using differential feeding mechanism.

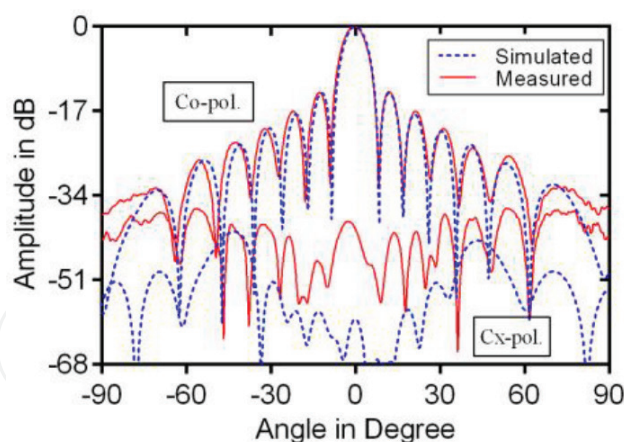


Figure 21. Simulated and measured radiation pattern of 2×10 planar SWA using differential feeding mechanism.

From **Figure 20**, it can be concluded that the planar array preserves the RL bandwidth of single linear array and the measured and simulated performances are in close match.

8. Conclusion

In this chapter, high efficiency broadband 10-element linear SWA integrated with differential feeding technique has been discussed in detail and also compared with conventional SWAs. The differential feeding technique has been proposed to eliminate the drawbacks of conventional SWAs excited with edge feeding and/or coupling slots. Mathematical justification of virtual short transpired due to differential feeding has also been presented and validated.

Ten-element linear SWAs employed with edge feeding, coupling slot feeding, and differential feeding have designed and simulated. The simulated results are also compared to validate the proposed advantages of differential feeding. About 7.5% return loss bandwidth has been achieved using differential feeding. Moreover, antenna efficiency and gain flatness performances are superior in the case of differential feeding. Presented designs of SWA are fabricated and characterized. In addition, 2×10 planar broadband SWA has also been designed, developed, and characterized. About 7.8% return loss bandwidth has been achieved in simulation. The measured performance of planar broadband SWA is also compared with simulated performance and good agreement has been achieved between them.

Furthermore, the proposed differential feeding techniques have shown many advantages like broad bandwidth, high power handling capacity, and the requirement of low fabrication tolerances. Therefore, this technique is the best suitable for SWA designs at millimeter wave and sub-millimeter wave.

Acknowledgements

The authors thank and appreciate the support and encouragement provided by Shri Tapan Misra, Director, SAC during the course of this work. The authors also wish to thank all

engineers of Microwave Sensors Antenna Division (MSAD) and Antenna Measurement Facility (AMF) for their help.

Author details

Yogesh Tyagi and Pratik Mevada*

*Address all correspondence to: pratik@sac.isro.gov.in

Microwave Sensors Antenna Division (MSAD), Space Applications Centre (SAC), Indian Space Research Organization (ISRO), Ahmedabad, India

References

- [1] Wang W, Zhong S-S, Zhang Y-M, Liang X-L. A broadband slotted ridge waveguide antenna array. *IEEE Transactions on Antennas and Propagation*. August 2006;**54**(8). DOI: 10.1109/TAP.2006.879216
- [2] Sekretarov SS, Vavriv DM. A wideband slotted waveguide antenna array for Sar systems. *Progress In Electromagnetics Research M*. 2010;**11**:165-176. DOI: 10.2528/PIERM10010606
- [3] Zhao HC, Xu RR, Wu W. Broadband waveguide slot array for SAR. *Electronics Letters*. January 2011;**47**(2). DOI: 10.1049/el.2010.3009
- [4] Silver S. *Microwave Antenna Theory and Design*. 1st ed. The United States of America: MacGraw-Hill Book Company, Inc.; 1949
- [5] David M. Pozar, *Microwave Engineering*. 3rd ed. Singapore: John Wiley & Sons, Inc.; 2005
- [6] Elliott RS, Kurtz LA. The Design of Small Slot Arrays. *IEEE Transactions on Antennas and Propagation*. March 1978;**AP-26**(2). DOI: 10.1109/TAP.1978.1141814
- [7] Elliott RS. An improved design procedure for small arrays of shunt slots. *IEEE Transactions on Antennas and Propagation*. January 1983;**AP-31**(1). DOI: 10.1109/TAP.1983.1143002
- [8] Kim DY, Elliott RS. A design procedure for slot arrays fed by single-ridge waveguide. *IEEE Transactions on Antennas and Propagation*. November 1988;**36**(11). DOI: 10.1109/8.9701

